

A study of 2-lobe symmetric hole entry hybrid journal bearing operating with non-Newtonian lubricant considering thermal effects

Prashant B. Kushare^{a,*}, Satish C. Sharma^{b,1}

^a Mechanical Engineering Department, K.K.Wagh Institute of Engineering Education and Research, Nashik-422003, India

^b Department of Mechanical and Industrial Engineering, Tribology Laboratory, Indian Institute of Technology, Roorkee, India

ARTICLE INFO

Article history:

Received 7 April 2015

Received in revised form

6 July 2015

Accepted 9 July 2015

Available online 17 July 2015

Keywords:

2-Lobe

Orifice

Cubic law

Hybrid

ABSTRACT

This paper presents the thermohydrostatic solution of 2-lobe symmetric hole entry hybrid journal bearing compensated with orifice restrictor and operating with cubic law lubricant. Simultaneous solutions of Reynold's, energy and conduction equations have been obtained by using finite element method and a suitable iterative scheme. The performance characteristics parameters of 2-lobe symmetric bearing system have been presented for various bearing geometries and nonlinearity factors. The numerically simulated results of the study indicates that the variation of viscosity of cubic law lubricant due to temperature rise and bearing geometry changes the bearing performance quite significantly.

© 2015 Elsevier Ltd. All rights reserved.

1. Introduction

The cylindrical non-recessed hybrid journal bearings are used extensively in various engineering applications owing to their superior dynamic performance characteristics [1–4]. However, the critical requirements pertaining to operating conditions necessitates these bearings to be designed more accurately. The circular non-recessed bearings are prone to fluid induced instabilities such as oil whirl and whip. This has necessitated the development of multilobe journal bearing to prevail over the fluid induced instabilities. Recently, many studies related to multilobe journal bearings have been carried out and reported in the published literature [5–10].

Furthermore, a lubricant plays a great role on the overall performance of bearings. Lubricants with high molecular weight polymeric additives such as polyisobutylene and polymethacrylate are extensively being used these days. These lubricants exhibit non-Newtonian behavior wherein, a non-linear relationship is observed between shear stress and rate of shear. Therefore, the performance of bearing simulated using Newtonian behavior postulations may not provide a realistic bearing design data.

During the last few decades, many studies [11–19] have been carried out in the field of circular hydrostatic/hybrid bearings

considering the non-Newtonian rheology of lubricants. Sinhasan and Sah [11] analytically investigated the influence of cubic law lubricant on the performance characteristics of circular hydrostatic journal bearing. The effect of nonlinear behavior of lubricant on flexible bearing system was carried out by Sharma et al. [12]. They reported that the nonlinear behavior of lubricant defined by a cubic shear stress law and a power law alters the dynamic response of a bearing system. Nagaraju et al. [14] studied the influence of roughness pattern on the performance of a hole entry hybrid journal bearing system lubricated with power law lubricant. They reported that the longitudinal surface pattern provides enhanced values of rotor dynamic coefficients for the value of power law index ($n=0.5$). Very recently, Kushare and Sharma [17,18] studied the influence of cubic law lubricant on the performance of two lobe worn hole entry journal bearing. They also presented the nonlinear transient stability response for the symmetric worn bearing configuration. It was reported that there is substantial reduction in the value of direct rotor dynamic coefficients of the order of 18–30% for worn bearing operated with cubic law lubricant.

Under the conditions of high speed and heavy operating load, temperature of lubricating fluid film and bearing surface increases. The rise in temperature changes the behavior of lubricant by reducing its viscosity. Further, as stated earlier, the addition of polymer additives changes the behavior of commercial lubricants to exhibit non-Newtonian behavior. Thus, the analysis based on the isothermal and isoviscous conditions of bearing operating with Newtonian lubricant may not provide realistic bearing performance. Therefore, to predict bearing performance characteristics

* Corresponding author. Mobile: +91 9890426679

E-mail addresses: pbkushare@gmail.com (P.B. Kushare), sshmefme@iitr.ernet.in (S.C. Sharma).

¹ Tel.: +91 1332 286609; fax: +91 1332 285665.

Nomenclature

a_b	bearing land width, mm
c	radial clearance, mm
e	journal eccentricity, mm
E	Young's modulus of elasticity, N mm ⁻²
F	fluid film reaction ($\partial h/\partial t \neq 0$), N
F_x, F_z	components of fluid film reactions in X and Z direction ($\partial h/\partial t \neq 0$), N
F_o	fluid film reaction ($\partial h/\partial t = 0$), N
C_1	clearance due to circumscribed circle on the bearing, mm
C_2	clearance due to inscribed circle on the bearing, mm
g	acceleration due to gravity, m s ⁻²
h	nominal fluid-film thickness, mm
L	bearing length, mm
R_j, R_L, R_b	radius of journal, lobe and bearing, mm
d_o	orifice diameter, mm
p	pressure, N mm ⁻²
p_c	pressure at hole, N mm ⁻²
Q	bearing flow, mm ³ s ⁻¹
S_{ij}	stiffness coefficients ($i, j = 1, 2$), N mm ⁻¹
C_{ij}	damping coefficients ($i, j = 1, 2$), N s mm ⁻¹
t	time, s
k	thermal conductivity, W mm ⁻¹ K ⁻¹
ω_l	(g/c) ^{1/2} , rad s ⁻¹
ψ_d	coefficient of discharge for orifice
D	journal diameter, mm
W_o	external load, N
Ω, Γ	solution domains
X, Y, Z	cartesian coordinates
X_j, Z_j	coordinates of steady state equilibrium journal center from geometric center of bearing, mm

Greek symbols

$\lambda = L/D$	aspect ratio
ϕ	altitude angle
μ	dynamic viscosity of lubricant, N s m ⁻²
μ_r	dynamic viscosity of lubricant at reference inlet temperature and ambient pressure, N s m ⁻²
ρ	density of the lubricant, kg mm ⁻³
K	nonlinearity factor for cubic shear law
τ	shear stress in lubricant film, N mm ⁻²
$\dot{\gamma}$	shear strain rate, s ⁻¹
μ_a	apparent viscosity, N s m ⁻²
O_j, O_{Li}	journal center, Lobe center
ω_j	journal rotational speed, rad s ⁻¹
ω_{th}	threshold speed, rad s ⁻¹
q	heat flux, W m ⁻²
p_s	lubricant supply pressure, N mm ⁻²

Non-dimensional parameters

$\bar{a}_b = a_b/L$	land width ratio
$\beta^* = p^*/p_s$	concentric design pressure ratio
$\bar{C}_{S2} = (\pi d_o^2 \mu \psi_d / 4c^3) (2/\rho p_s)^{1/2}$	restrictor design parameter
$\bar{D}_e = \left(\frac{\mu_r}{\rho_j c_{pf}} \right) \left(\frac{c^2 p_s}{\mu_r R_j} \right) \frac{R_j}{c^2 T_r}$	

\bar{u}, \bar{v}	$(u, v) \left(\frac{\mu_r R_j}{c^2 p_s} \right)$
\bar{C}_{ij}	$C_{ij} \left(\frac{c^3}{\mu R_j^4} \right)$
\bar{F}, \bar{F}_o	$(F, F_o) / p_s R_j^2$
\bar{h}	$(h)/c$; $\bar{\delta}_w = \delta_w/c$
$\bar{p}, \bar{p}_c, \bar{p}_{max}$	$(p, p_c, p_{max})/p_s$
\bar{Q}	$Q/(c^3 p_s)$
\bar{T}	T/T_r
$\bar{\gamma}$	$(\dot{\gamma})/(c p_s / \mu_r R_j)$
\bar{t}_b	$\frac{t_b}{R_j}$
\bar{K}	$(c p_s / R_j)^2 K$
\bar{k}	k/k_r
\bar{S}_{ij}	$S_{ij} (c/p_s R_j^2)$
\bar{W}_o	$W_o/p_s R_j^2$
(\bar{X}_j, \bar{Z}_j)	$(X_j, Z_j)/c$
$\bar{\tau}$	$t \left(\frac{c^2 p_s}{\mu R_j^2} \right)$
\bar{X}_L^i, \bar{Z}_L^i	$(X_L^i, Z_L^i)/c$
$\alpha, \beta = (X, Y)/R_j$	circumferential and axial coordinates
$\varepsilon = e/c$	eccentricity ratio
$\delta = C_1/C_2$	offset factor
$\bar{\omega}_{th}$	ω_{th}/ω_l
$\Omega = \omega_j \left(\mu R_j^2 / c^2 p_s \right)$	speed parameter

Matrices

N_i, N_j	shape functions
$[\bar{F}]$	fluidity matrix
$\{\bar{p}\}$	nodal pressure vector
$\{\bar{Q}\}$	nodal flow vector
$\{\bar{R}_H\}$	vector due to hydrodynamic terms
$\{\bar{R}_{Xj}\}, \{\bar{R}_{Zj}\}$	right hand side vectors due to journal center velocities
$[\bar{K}_T]$	system thermal stiffness matrix for solid (bush) domain
$[\bar{K}_h]$	system thermal stiffness matrix due to convection term for solid (bush) domain
$\{\bar{H}_T\}$	nodal heat flow vector
$[\bar{A}_T]$	system thermal stiffness matrix for fluid domain
$[\bar{B}_T]$	nodal thermal load vector for fluid domain
$[\bar{C}_T]$	vector representing the interaction with the bush and journal
$\{\bar{T}_f\}$	nodal fluid-film temperature vector
$\{\bar{T}_b\}$	nodal bush temperature vector

Subscripts and superscripts

b	bearing
R	restrictor
l	lobe
min	minimum
.	first derivative w.r.t time
*	concentric operation
j	journal
s	supply
i	lobe number
max	maximum
..	second derivative w.r.t time
-	corresponding non-dimensional parameter
r	reference value

realistically, thermohydrostatic analysis with non-Newtonian lubricant must be considered.

In recent times researchers have given considerable attention to thermal effects. Many studies related to thermohydrodynamic/

thermohydrostatic analyses pertaining to circular journal bearings have been reported in the literature [20–30]. Study pertaining to the influence of thermal effects on the performance of finite length journal bearing was carried out by Ferron et al. [21]. They obtained

the solution of generalized Reynold's equation, energy and conduction equations. They carried out theoretical and experimental comparative study of effect of viscosity variation due to temperature. Prashad [22] studied the performance of hydrodynamic journal bearing by considering the effects of clearance and viscosity variation for different lubricating oils. He proposed a more pragmatic method for the design and performance assessment of a bearing. Khonsari et al. [23] presented a simple way of predicting the maximum operating temperatures of pad surface and the journal surface by using thermohydrodynamic design chart. A thermo-elastohydrodynamic study of grooved hydrodynamic journal bearing was carried out by Sinhasan and Chandrawat [24]. Fillon and Bouyer [26] investigated the thermohydrodynamic performance characteristics of worn out plain journal bearing. The results of the studies demonstrated a significant deterioration in bearing performance characteristics due to thermal effects. Kumar et al. [27] reported the influence of thermal effect on the static performance of non-recessed circular hybrid journal bearing system. Very recently, Garg et al. [29] examined the influence of nonlinear behavior of lubricant due to the addition of additives and rise in temperature of fluid film on the performance of circular multiple entry journal bearing. Further, they [30,34] investigated the effect of temperature rise on performance of circular non-recessed hybrid journal bearing compensated with different types of restrictors. The results of the studies [29,30,34] indicate that the performance of journal bearings is affected quite significantly because of temperature rise of lubricant film. Therefore, it becomes imperative to consider the thermal effect in the analysis to envisage the factual performance of bearing system.

A thorough scan of the literature reveals that the performance of journal bearings is greatly dependent on the influence of thermal effects and non-Newtonian behavior of lubricant. The survey of available literature also indicates that the majority of the studies of hybrid journal bearings operated with non-Newtonian lubricants are based on isothermal assumption. However, no study has yet been reported in the literature that deals with the thermohydrostatic analysis of 2-lobe symmetric hybrid journal bearing. Therefore, the present study is aimed to carry out the thermohydrostatic analysis of 2-lobe symmetric hole entry hybrid journal bearing operating with cubic law lubricant so as to evaluate realistic bearing characteristics data. Furthermore, thermohydrostatic performance comparison of a 2-lobe bearing and circular bearing configurations has also been presented for Newtonian and cubic law lubricant. Geometry of 2-lobe symmetric hybrid journal bearing system used in the analysis is shown in Fig. 1.

2. Generalized Reynolds equation for non-newtonian lubricant fluid field

The modified form of Reynolds equation governing the flow of non-Newtonian lubricant flow field (laminar and incompressible) for 2-lobe journal bearing is expressed in non-dimensional form as [13,18,29–31,34]

$$\frac{\partial}{\partial \alpha} \left(\bar{h}^3 \bar{F}_2 \frac{\partial \bar{p}}{\partial \alpha} \right) + \frac{\partial}{\partial \beta} \left(\bar{h}^3 \bar{F}_2 \frac{\partial \bar{p}}{\partial \beta} \right) = \Omega \left[\frac{\partial}{\partial \alpha} \left\{ \left(1 - \frac{\bar{F}_1}{\bar{F}_0} \right) \bar{h} \right\} \right] + \frac{\partial \bar{h}}{\partial t} \quad (1)$$

where \bar{F}_0 , \bar{F}_1 , and \bar{F}_2 are the cross film viscosity integrals and are defined as

$$\bar{F}_0 = \int_0^1 \frac{1}{\bar{\mu}} d\bar{z}, \bar{F}_1 = \int_0^1 \frac{\bar{z}}{\bar{\mu}} d\bar{z}, \bar{F}_2 = \int_0^1 \frac{\bar{z}^2}{\bar{\mu}} d\bar{z} \quad (2)$$

2.1. Cubic law fluid model

The non-linear relation between shear stress and shear strain rate of most of the polymer-thickened oils or lubricants are adequately

defined and characterized by the cubic law fluid model [11,12,15–19]. The cubic law fluid model is defined in non-dimensional form by the following relations [11,15,18,29,34]:

$$\bar{\tau} + \bar{K} \bar{\tau}^3 = \bar{\gamma} \quad (3)$$

The viscosity of a cubic law lubricant is defined by the apparent viscosity ($\bar{\mu}_a$) in terms of shear strain rate and is expressed as

$$\bar{\mu}_a = \bar{\tau} / \bar{\gamma} \quad (4)$$

For an incompressible non-Newtonian lubricant film, the shear strain rate ($\dot{\gamma}$) is expressed as [11,15,30]

$$\bar{\gamma} = \left[\left(\left[\frac{\bar{h}}{\bar{\mu}} \frac{\partial \bar{p}}{\partial \alpha} \left(\bar{z} - \frac{\bar{F}_1}{\bar{F}_0} \right) + \frac{\Omega}{\bar{\mu} \bar{h} \bar{F}_0} \right] \right)^2 + \left(\left[\frac{\bar{h}}{\bar{\mu}} \frac{\partial \bar{p}}{\partial \beta} \left(\bar{z} - \frac{\bar{F}_1}{\bar{F}_0} \right) \right] \right)^2 \right]^{1/2} \quad (5)$$

2.2. Restrictor flow equations

The flow of cubic law lubricant for a 2-lobe symmetric journal bearing through an orifice restrictor (\bar{Q}_R) in non-dimensional form is expressed as [11,12,29,33]

$$\bar{Q}_R = \bar{C}_{s2} (1 - \bar{p}_c)^{1/2} \quad (6)$$

2.3. Lubricant flow field boundary conditions

The boundary conditions relevant to the lubricant flow field are described as [11,18,29,33,34]

1. At the external boundary, nodal pressures are zero.
2. All nodes situated on holes have equal pressure.
3. At the trailing edge of the positive region, $\bar{p} = (\partial \bar{p} / \partial \alpha) = 0.0$ Swift–Stieber cavitation condition.

2.4. Temperature viscosity relation

The temperature dependent viscosity of the fluid is defined by the following relation in non-dimensional form [20,21,26,27]:

$$\bar{\mu} = \frac{\mu}{\mu_r} = \exp \left[\bar{a}_1 \left[\frac{1 + 273.12 / T_r}{\bar{T}_f + 273.12 / T_r} - 1 \right] \right] \quad (7)$$

2.5. Fluid film temperature distribution

The 3-D energy equation is used to obtain fluid-film temperature distribution in the fluid domain and is written in non-dimensional form as [20,21,23,25–27,34]

$$\bar{h}^2 \left[\bar{u} \frac{\partial \bar{T}_f}{\partial \alpha} + \bar{v} \frac{\partial \bar{T}_f}{\partial \beta} + \frac{\bar{w}}{\bar{h}} \frac{\partial \bar{T}_f}{\partial \bar{z}} \right] = \bar{P}_e^* \left(\frac{\partial^2 \bar{T}_f}{\partial \bar{z}^2} \right) + \bar{D}_e \bar{\mu} \left[\left(\frac{\partial \bar{u}}{\partial \bar{z}} \right)^2 + \left(\frac{\partial \bar{v}}{\partial \bar{z}} \right)^2 \right] \quad (8)$$

where \bar{P}_e^* and \bar{D}_e are inverse Peclet and dissipation numbers and are defined as

$$\bar{P}_e^* = \left(\frac{k_r}{\rho_f c_{pf}} \right) \left(\frac{\mu_r R_j}{c^2 p_s} \right) \frac{R_j}{c^2} \quad (8.1)$$

$$\bar{D}_e = \left(\frac{\mu_r}{\rho_f c_{pf}} \right) \left(\frac{c^2 p_s}{\mu_r R_j} \right) \frac{R_j}{c^2 T_r} \quad (8.2)$$

The discretization of the entire fluid domain is done by using eight node hexahedral linear isoparametric elements. The 3-dimensional finite element grid used for the thermal analysis is made compatible for 2-dimensional grid for lubrication flow field i.e., 2D mesh of the lubrication domain is the projection of the 3D mesh of the thermal domain. The distributions of temperatures and velocity components

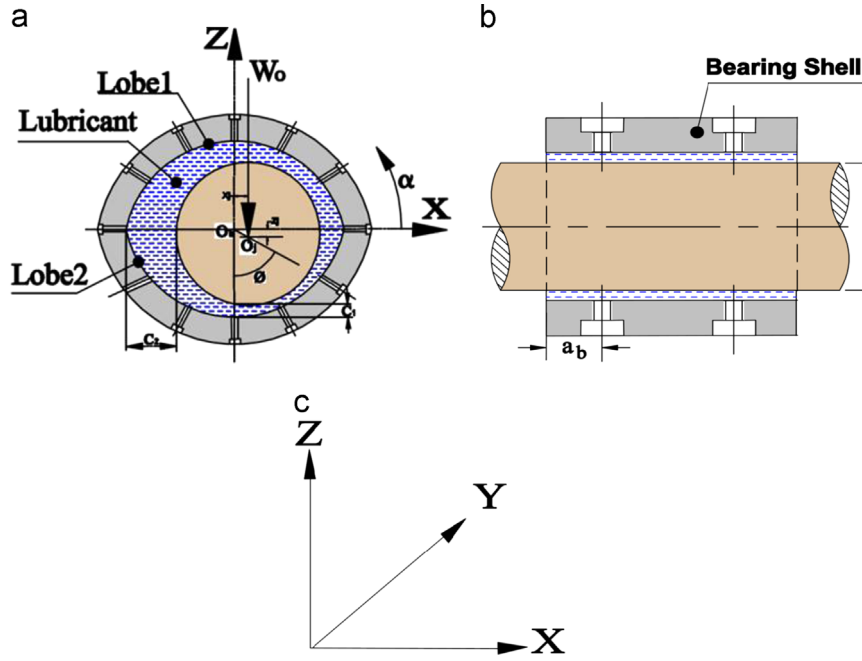


Fig. 1. Geometry of symmetric 2-lobe hole entry hybrid journal bearing.

over an eth element are expressed as [25,27]

$$\bar{T}_f^e = \sum_{j=1}^{n_e^e} \bar{T}_{ffj} N_j \quad (9)$$

$$\bar{u}, \bar{v}, \bar{w} = \sum_{j=1}^{n_e^e} (\bar{u}_j, \bar{v}_j, \bar{w}_j) N_j \quad (10)$$

Using Galerkin's method Eq. (8) is reduced to the following system equation:

$$[\bar{A}_T] \{\bar{T}_f\} = \{\bar{B}_T\} + \{\bar{C}_T\} \quad (11)$$

The system Eq. (11) is obtained by assembling the contribution of all elements in the entire discretized fluid domain, where for an eth element:

$$\bar{A}_{Tij}^e = \int_{\Omega^e} \left[N_i \bar{h}^2 \left(\bar{u} \frac{\partial N_j}{\partial \alpha} + \bar{v} \frac{\partial N_j}{\partial \beta} + \bar{w} \frac{\partial N_j}{\partial \bar{z}} \right) + \bar{P}_e^* \frac{\partial N_i}{\partial \bar{z}} \frac{\partial N_j}{\partial \bar{z}} \right] d\Omega^e \quad (11.1)$$

$$\bar{B}_{Tij}^e = \bar{D}_e \int_{\Omega^e} \left[\left\{ \sum_{j=1}^{n_e^e} \left(\frac{\partial N_j}{\partial \bar{z}} \cdot \bar{u}_j \right)^2 \right\} + \left\{ \sum_{j=1}^{n_e^e} \left(\frac{\partial N_j}{\partial \bar{z}} \cdot \bar{v}_j \right)^2 \right\} \right] N_i d\Omega^e \quad (11.2)$$

$$\bar{C}_{Ti} = \bar{P}_e^* \int_{\Gamma^e} \frac{\partial \bar{T}_f}{\partial \bar{z}} N_i d\Gamma^e \quad (11.3)$$

2.6. Temperature distribution in the bush

The 3-D Fourier heat conduction equation is applied to establish the temperature distribution in the bush. In cylindrical co-ordinate system, the heat transfer equation is written in non-dimensional form as [21,23,25,32,34]

$$\frac{1}{\bar{r}} \frac{\partial}{\partial \bar{r}} \left(\bar{k}_b \bar{r} \frac{\partial \bar{T}_b}{\partial \bar{r}} \right) + \frac{1}{\bar{r}^2} \frac{\partial}{\partial \alpha} \left(\bar{k}_b \frac{\partial \bar{T}_b}{\partial \alpha} \right) + \bar{r} \frac{\partial}{\partial \beta} \left(\bar{k}_b \frac{\partial \bar{T}_b}{\partial \beta} \right) = 0 \quad (12)$$

For thermal analysis of fluid domain and the bush, the compatibility of discretized bush grid (8-node hexahedral isoparametric elements) is made with the one used for lubrication. The bush

temperature (\bar{T}_b) distribution over an eth element is expressed as

$$\bar{T}_b = \sum_{j=1}^{n_e^e} N_j \bar{T}_{bj} \quad (13)$$

Using Galerkin's technique, the following system equation in assembled form is obtained:

$$[[\bar{K}_T] + [\bar{K}_h]] \{\bar{T}_b\} = \{\bar{H}_T\} \quad (14)$$

where for eth element:

$$[\bar{K}_T]^e = \int_{\Omega^e} \left(\bar{k}_b \left(\frac{1}{\bar{r}^2} \frac{\partial N_i}{\partial \alpha} \frac{\partial N_j}{\partial \alpha} + \bar{r} \frac{\partial N_i}{\partial \beta} \frac{\partial N_j}{\partial \beta} + \frac{\partial N_i}{\partial \bar{r}} \frac{\partial N_j}{\partial \bar{r}} \right) \right) d\Omega^e \quad (14.1)$$

$$[\bar{K}_h]^e = \int_{\Gamma^e} \bar{h}_b N_i N_j d\Gamma^e \quad (14.2)$$

$$\{\bar{H}_T\}^e = \int_{\Gamma^e} \bar{q} N_i d\Gamma^e \quad (14.3)$$

In Eqs. (14.1)–(14.3), Ω^e corresponds to the inside domain of element 'e' and Γ^e corresponds to the boundary of element 'e'.

2.7. Boundary conditions on the temperature

The solution of energy equation and conduction equation is obtained by using the relevant boundary conditions [21,25,30,32,34]:

1. Fluid-film journal interface, $\bar{T}_f = \bar{T}_j$ at $\bar{z} = 1.0$ and fluid-film bush interface, $\bar{T}_f = \bar{T}_b$ at $\bar{z} = 0.0$
2. On the fluid-bush interface to maintain continuity of the heat flux:

$$-\bar{k}_b \left(\frac{\partial \bar{T}_b}{\partial \bar{r}} \right) \bigg|_{\bar{r} = \bar{R}_1} = \frac{\bar{k}_f}{\bar{c} \bar{h}} \left(\frac{\partial \bar{T}_f}{\partial \bar{z}} \right) \bigg|_{\bar{z} = 0}$$

3. On the external surface of the bush for free convection:

$$\frac{\partial \bar{T}_b}{\partial \bar{r}} \bigg|_{\bar{r} = R_2} = -\frac{h_b t_h}{k_b} (\bar{T}_b|_{\bar{r} = R_2} - \bar{T}_a)$$

4. On the lateral faces of the bearing ($\beta = \pm \lambda$):

$$\frac{\partial \bar{T}_b}{\partial \beta} \Big|_{\beta = \pm \lambda} = -\frac{h_b R}{k_b} (\bar{T}_b \Big|_{\beta = \pm \lambda} - \bar{T}_a)$$

2.8. Stability parameters

Using Rouths' criteria, the stability parameters of journal bearing system are defined subsequently. The non-dimensional critical mass \bar{M}_c of the journal is expressed as [17,18]

$$\bar{M}_c = \frac{\bar{G}_1}{\bar{G}_2 - \bar{G}_3} \quad (15)$$

where

$$\bar{G}_1 = [\bar{C}_{xx} \bar{C}_{zz} - \bar{C}_{zx} \bar{C}_{xz}] \quad (15.1)$$

$$\bar{G}_2 = \frac{[\bar{S}_{xx} \bar{S}_{zz} - \bar{S}_{zx} \bar{S}_{xz}] [\bar{C}_{xx} + \bar{C}_{zz}]}{[\bar{S}_{xx} \bar{C}_{zz} + \bar{S}_{zz} \bar{C}_{xx} - \bar{S}_{xz} \bar{C}_{zx} - \bar{S}_{zx} \bar{C}_{xz}]} \quad (15.2)$$

$$\bar{G}_3 = \frac{[\bar{S}_{xx} \bar{C}_{xx} + \bar{S}_{xz} \bar{C}_{xz} + \bar{S}_{zx} \bar{C}_{zx} + \bar{S}_{zz} \bar{C}_{zz}]}{[\bar{C}_{xx} + \bar{C}_{zz}]} \quad (15.3)$$

Threshold speed can be obtained using the relation given below:

$$\bar{\omega}_{th} = [\bar{M}_c / \bar{F}_0]^{1/2} \quad (15.4)$$

where \bar{F}_0 is the resultant fluid-film force or reaction. $(\partial \bar{h} / \partial \bar{t}) = 0$

3. Solution procedure

To establish the solution of fluid film pressure and fluid film temperature field for a 2-lobe symmetric hybrid journal bearing and a simultaneous solution of Reynolds equation, heat transfer equation (energy equation, conduction equation) and orifice restrictor flow equation along with suitable boundary condition requires an iterative solution scheme. An Overall iterative procedure used to obtain the converged solution mainly consists of four

different block units; viz. PRES, non-NEWTN, ENGY and CNDC as shown in Fig. 2 and which is briefly described as follows:

1. The input data for pressure and temperature field is read in unit PDATA.
2. In block non-NEWTN, the values of cross viscosity integrals \bar{F}_0, \bar{F}_1 and \bar{F}_2 , at each Gauss point are computed to get the value of fluid-film viscosity for both Newtonian and cubic law lubricants.
3. The initial trial solution of Newtonian lubricant is used for the cubic law lubricant. The apparent viscosity ($\bar{\mu}_a$) is computed by using Eq. (4) of the shear strain rate ($\bar{\gamma}$) and Eq. (5) shear stress ($\bar{\tau}$).
4. The iterations of convergence are terminated when the required pressure of the flow field satisfies the required tolerance limit criterion. When the difference in nodal pressures at each node in the successive iteration becomes less than the predefined tolerance of $ZO \leq 0.001$:

$$\left| \frac{\{\bar{p}^m\} - \{\bar{p}^{(m-1)}\}}{\{\bar{p}^{(m-1)}\}} \right| \times 100 \leq 0.001 \quad (16)$$

5. In block PRES, the solution of system equations are obtained to get the fluid-film pressures by using appropriate boundary condition.
6. The Block ENGY solves the energy equation (Eq. (8)) along with appropriate boundary conditions. If a specified criterion about temperature is not specified, the boundary condition at the fluid bush interface is modified in unit TBN DY to solve energy equation.
7. In order to obtain the temperature distribution over the solution domain, nodal pressures computed in PRES block are used to compute the fluid velocity components. An iterative solution scheme is employed to solve the energy equation for obtaining the fluid film temperatures.
8. The obtained fluid film temperatures are used to establish the journal temperature. The iterative procedure is terminated when the temperature at all the nodes of the flow field satisfies the following convergence criterion [16,25,34]:

$$\left| \frac{\{\bar{T}_J^m\} - \{\bar{T}_J^{(m-1)}\}}{\{\bar{T}_J^{(m-1)}\}} \right| \times 100 \leq 0.001 \quad (17)$$

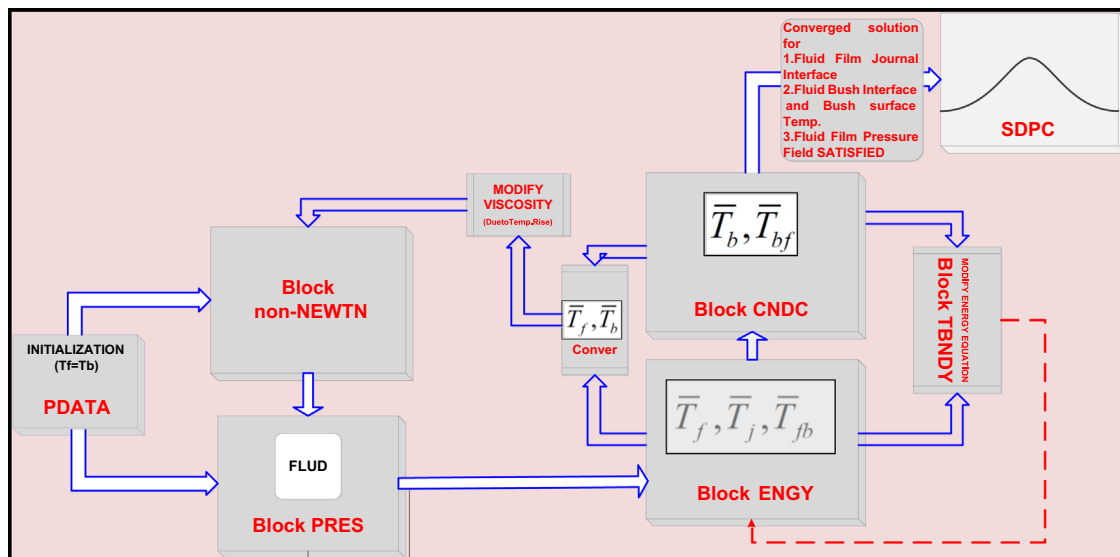


Fig. 2. Overall iterative solution procedure.

9. The fluid-film temperatures so obtained are used as boundary conditions for solving the conduction equation. In block CNDC, a 3-dimensional heat conduction equation is solved to get the temperature distributions in the bush.
10. The prescribed temperature boundary conditions are to be read from the data file generated from the solution of the energy equation. A check for the convergence on the fluid bush interface temperature is employed.
11. The temperature distribution obtained in the bush is used to ascertain the fluid bush interface temperature. The fluid-film temperatures are used to modify the viscosity of the fluid-film to compute the pressure field for the next iteration.
12. The iterations are terminated when the nodal pressures of flow field satisfies the criterion expressed by Eq. (15).
13. Unit SDPC is used to compute the bearing performance characteristics.

4. Results and discussion

The performance characteristics of a 2-lobe symmetric hybrid journal bearing system have been obtained by using the analysis and solution procedure mentioned in the preceding section. The influence of temperature rise is accounted by defining and computing the value of inverse Peclet number (P_e^*) and dissipation number (\bar{D}_e) from lubricant properties. The value of bearing geometric and operating parameters have been chosen from the already published literature [1,3,9–12,14,18,21,25,27,32] on the basis of their broad applicability and is given in Table 1. As stated earlier, no thermohydrostatic results are available in the published literature for 2-lobe symmetric hybrid journal bearing. Thus, to authenticate solution algorithm and developed numeric model, the computed results for circular bearings from the present analysis are validated and compared with the earlier published results [15,21] for the case of thermal effects and non-Newtonian lubricant. For thermal effect, the

results have been computed for hydrodynamic circular journal bearing system and compared with the published results of Ferron et al. [21] as shown in Fig. 3. The identical operating conditions of theoretical work of Ferron et al. were chosen in the present work. This result agrees quite well for both theoretical as well as experimental study results of Ferron et al. [21]. The difference in results may be attributed to the use of different computational schemes. Further, the result for influence of non-Newtonian lubricant on the performance of hydrodynamic journal bearing is compared with the results of Wada and Hayashi [15]. The results matches well as shown in Fig. 4. The thermohydrostatic analysis on the performance of a 2-lobe symmetric hole entry hybrid journal bearing operating with cubic law lubricant have been performed. The computed bearing performance characteristics such as \bar{h}_{min} , \bar{Q} , \bar{S}_{11} , \bar{S}_{22} , \bar{C}_{11} , \bar{C}_{22} and $\bar{\omega}_{th}$ have been presented through Figs. 5–9 for different values the offset

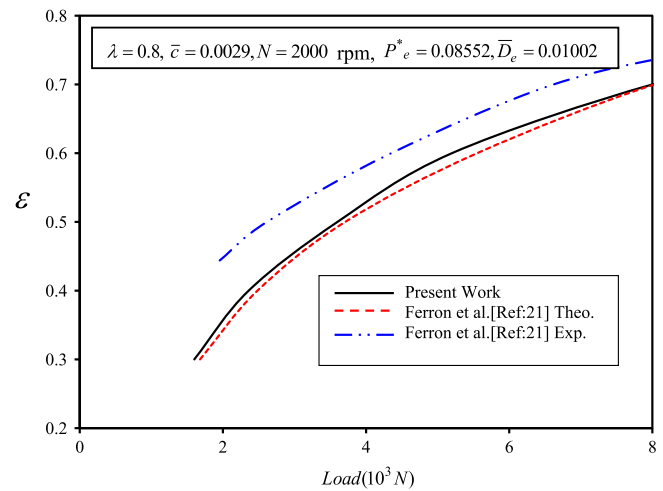


Fig. 3. Variation of eccentricity ratio (ϵ) with load.

Table 1
Bearing geometric and operating data [1,3,9,10–12,14,18,21,25,27,32].

Bearing geometric parameter	2-Lobe symmetric hole entry hybrid journal bearing		Unit
Journal radius	R_j	50	mm
Bush external radius	R_2	55	mm
Radial clearance	c	0.05020	mm
Bearing length	L	100	mm
Bush thickness	t_b	5	mm
Land width ratio	a_b/L	0.25	dimensionless
Lubricant characteristics			
Specific heat	C_p	2000	J kg ⁻¹ K ⁻¹
Density	ρ_f	858	kg m ⁻³
Thermal conductivity	k_f	0.125	W m ⁻¹ K ⁻¹
Viscosity (at 40 °C)	μ_f	0.0345	Pa s
Solid characteristics			
Thermal conductivity of bush	k_b	50	W m ⁻¹ K ⁻¹
Modulus of elasticity of bush	E_b	0.524	N mm ⁻²
Poisson's ratio of bush	ν_b	0.357	dimensionless
Operating parameters			
Journal speed	N	2500	rpm
External load	W_o	22.4	kN
Offset factor	δ	0.9,1.0,1.1	dimensionless
Non-linearity factor	\bar{K}	0.0,0.58,1.0	dimensionless
Supply pressure	p_s	8.96×10^6	N m ⁻²
Supply temperature	T_s	40	°C
Ambient temperature	T_a	40	°C
Other parameters			
Convection heat transfer coefficient between bush and air	h_b	50	W m ⁻² K ⁻¹
Thermal conductivity of air	k_a	0.025	W m ⁻¹ K ⁻¹
Density of the air	ρ_a	1.3	kg m ⁻³
Specific heat of air	c_{pa}	1005	J kg ⁻¹ K ⁻¹
Viscosity of air	μ_a	0.002	Pa s

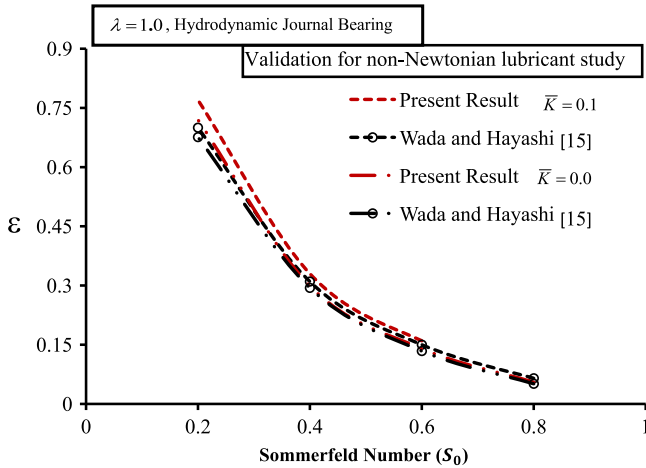


Fig. 4. Variation of Eccentricity ratio (ϵ) with Sommerfeld number (S_0).

factor (δ) and nonlinearity factor (\bar{K}). The comparative study of the isothermal (IHS) and thermal (THS) condition is also presented in terms of minimum fluid film thickness (\bar{h}_{min}), direct fluid film stiffness coefficients (\bar{S}_{22}) and stability threshold speed margin ($\bar{\omega}_{th}$).

4.1. Minimum fluid film thickness (\bar{h}_{min})

Fig. 5(a) depicts the variation of minimum fluid film thickness (\bar{h}_{min}) for 2-lobe symmetric bearing system. The value of minimum fluid-film thickness \bar{h}_{min} gets reduced when bearing operates with cubic law lubricant. The value of \bar{h}_{min} is found to reduce with an increase in the value of nonlinearity factor (\bar{K}). This is due to the fact that the temperature rise in fluid film results in nonlinear behavior of lubricant, which decreases the viscosity of the lubricant. As a result of this, increased rate of deformation of fluid film makes film thinner and bearing operates at lower values of \bar{h}_{min} for cubic law lubricant. Furthermore, it may also be observed that the values of minimum fluid film thickness (\bar{h}_{min}) decreases as the value of offset factor (δ) increases. The maximum reduction in the value of \bar{h}_{min} due to thermal effect and cubic law lubricant at offset factor ($\delta > 1.0$) is found to the order of 12–14% when compared with circular bearing operating with Newtonian lubricant ($\bar{K} = 0.0$).

Fig. 5(b) indicates the variation of \bar{h}_{min} for IHS and THS case. From Fig. 5(b), it has been observed that for IHS (isothermal) condition, the bearing operates at higher values of minimum fluid film thickness than that for THS case. Whereas, in THS case, the combined influence of bearing geometry and nonlinear behavior of cubic law lubricant (\bar{K}) substantially lowers the value of (\bar{h}_{min}). Thus, in order to maintain a safe operating value of \bar{h}_{min} , a proper selection of values of noncircular bearing profile (offset factor) and nonlinearity factor (\bar{K}) is essential. For THS condition, a value of operating external load $\bar{W}_0 = 1.2$, the value of minimum fluid film thickness (\bar{h}_{min}) gets reduced by 5% with respect to IHS (isothermal) condition. As indicated through the points A–A' of Fig. 5(b), the maximum decrease in the value of fluid film thickness (\bar{h}_{min}) is observed to the order of 4% for THS condition due to the temperature and shear thinning behavior of changed viscosity at $\delta = 1.1$, $\bar{W}_0 = 1.2$ and $\bar{K} = 1$ with respect IHS (isothermal) condition at $\bar{K} = 0.0$.

4.2. Direct fluid-film stiffness coefficients (\bar{S}_{11} , \bar{S}_{22})

Fig. 6(a) and (b) depicts the variation of direct fluid film stiffness coefficients ($\bar{S}_{11}/\bar{S}_{22}$) computed for symmetric 2-lobe hole entry hybrid journal bearings. It may be noticed that the value of direct fluid film stiffness coefficient ($\bar{S}_{11}/\bar{S}_{22}$) gets reduced due to thermal

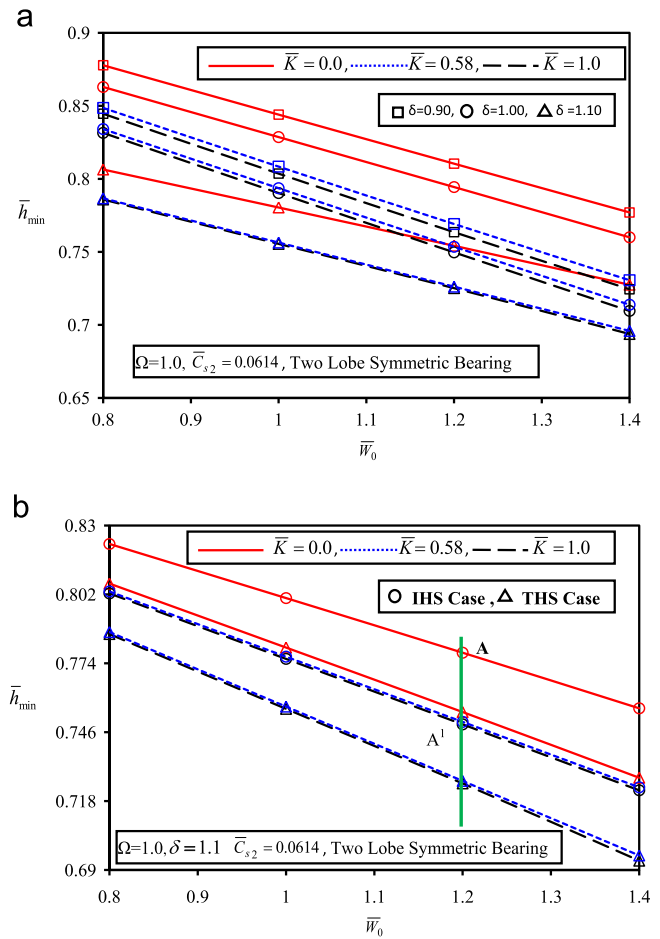


Fig. 5. (a) Variation of \bar{h}_{min} . (b) Variation of \bar{h}_{min} for IHS and THS case.

effects (THS) and increase in the value of nonlinearity factor \bar{K} . The combined influence of viscosity variation due to temperature rise and nonlinear behavior of the lubricant have a significant effect on the value of direct fluid film stiffness coefficients ($\bar{S}_{11}/\bar{S}_{22}$). Because of this, a reduction in the value of $\bar{S}_{11}/\bar{S}_{22}$ is observed of the order of 4% and 6% respectively at the value of offset factor $\delta = 1.1$ than that of circular profile journal bearing ($\delta = 1.0$) operating with Newtonian lubricant. Further, it may also be revealed that the noncircular bearing geometry ($\delta > 1.0$) provides higher value of direct fluid film stiffness coefficients ($\bar{S}_{11}/\bar{S}_{22}$) than the circular bearing for the same operating condition. At a given value of external load, thermohydrostatic analysis provides a higher value of \bar{S}_{22} than the value of \bar{S}_{11} for symmetric bearing configuration. The variation in the value of \bar{S}_{22} in both isothermal (IHS) and thermal (THS) case at the value of offset factor $\delta = 1.1$ is presented in Fig. 6(c). The influence of nonlinear behavior of the lubricant $\bar{K} = 1.0$ shows substantial effect for THS condition thereby decreasing the value of \bar{S}_{22} than the IHS (isothermal) case of 2-lobe hole entry bearing configuration. In case of THS, the nonlinearity factor $\bar{K} = 1.0$ and $\bar{K} = 0.58$ have a crucial influence on the value of \bar{S}_{22} . The reduction in the value of \bar{S}_{22} is found to the order of 11% due to temperature rise at $\bar{K} = 1.0$. This is due to shear thinning effect caused by temperature viscosity variation and which makes the film less stiff.

For bearing configuration operating with Newtonian lubricant $\bar{K} = 0.0$, the maximum reduction in the value of \bar{S}_{22} is found to be of the order of 13% for THS condition when compared with IHS (isothermal) condition as indicated in Fig. 6(c) through the points B–B'.

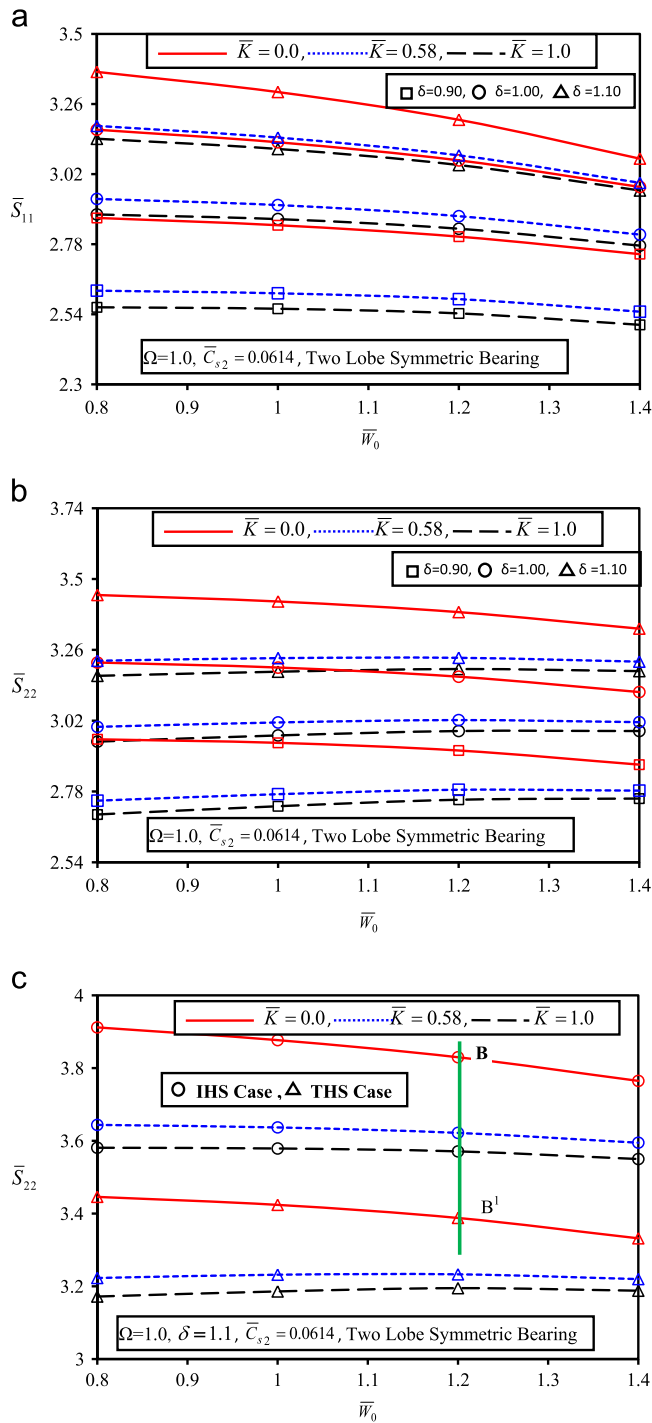


Fig. 6. (a) Variation of \bar{S}_{11} . (b) Variation of \bar{S}_{22} . (c) Variation of \bar{S}_{22} for IHS and THS case.

4.3. Direct fluid-film damping coefficient ($\bar{C}_{11}/\bar{C}_{22}$)

Fig. 7(a) and (b) shows the variation in direct fluid-film damping coefficient (\bar{C}_{11} and \bar{C}_{22}) due to thermal and non-Newtonian effects in case of 2-lobe symmetric non-recessed journal bearing system. From Fig. 7(a) and (b), it is noticed that the value of $\bar{C}_{11}/\bar{C}_{22}$ increases for 2-lobe symmetric bearing configuration when Newtonian lubricants are used. Further, reduction in the value of $\bar{C}_{11}/\bar{C}_{22}$ is observed when it is operated with non-Newtonian lubricants. For same operating condition, the nonlinearity factor shows significant reduction in the value of \bar{C}_{11} than \bar{C}_{22} .

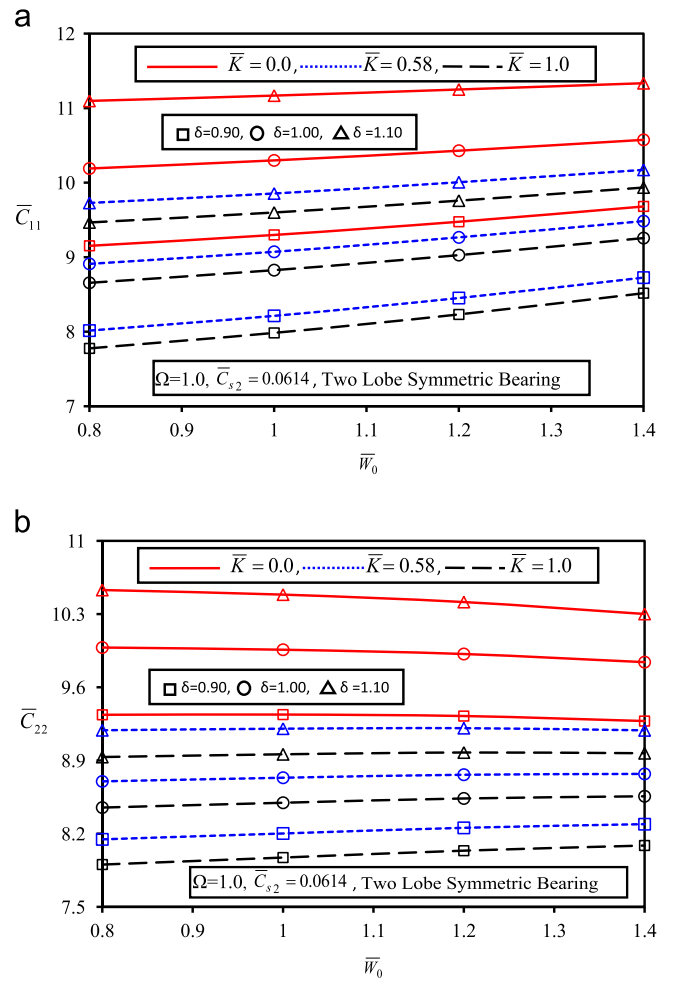


Fig. 7. (a) Variation of \bar{C}_{11} . (b) Variation of \bar{C}_{22} .

Further, it has been noticed from Fig. 7(b) that the circular as well 2-lobe non-recessed compensated bearing is to reduce the value of damping in vertical direction (\bar{C}_{22}) when operate with cubic law lubricant ($\bar{K}=1.0$). The bearing operating with Newtonian lubricant provides a higher value of $\bar{C}_{11}/\bar{C}_{22}$ than that of cubic law lubricant operated bearing. Further, it may be revealed that the value of $\bar{C}_{11}/\bar{C}_{22}$ increases with increase in the value of δ . From Fig. 7(a) and (b); it may be clearly noticed that the loss occurred in direct damping $\bar{C}_{11}/\bar{C}_{22}$ due to $\bar{K}=1.0$, $\bar{K}=0.58$ is partially compensated by 2-lobe non-recessed bearing configuration at the value of offset factor $\delta > 1.0$. For the sake of brevity, the results of the comparison of THS and IHS case are not presented here for \bar{C}_{11} and \bar{C}_{22} . For THS case, non-Newtonian lubricated bearing $\bar{K}=1.0$, the value of \bar{C}_{11} is observed to reduce by the order of nearly 20% whereas, the value of \bar{C}_{22} is reduced in the order of 22.2% at the value of offset factor $\delta=1.1$. Further, it is found that for lobed bearing configuration ($\delta > 1.0$), the value of \bar{C}_{11} and \bar{C}_{22} is enhanced by 11.14% and 7% respectively than circular non-recessed journal bearing.

4.4. Stability threshold speed margin ($\bar{\omega}_{th}$)

The variation of stability threshold speed margin ($\bar{\omega}_{th}$) is shown in Fig. 8(a). The stability threshold speed margin ($\bar{\omega}_{th}$) starts decreasing with an increase in the value of nonlinearity factor (\bar{K}). The dynamic response due to temperature rise and nonlinear rheology of cubic law lubricant is observed to decrease the value of stability threshold speed margin ($\bar{\omega}_{th}$) substantially for 2-lobe

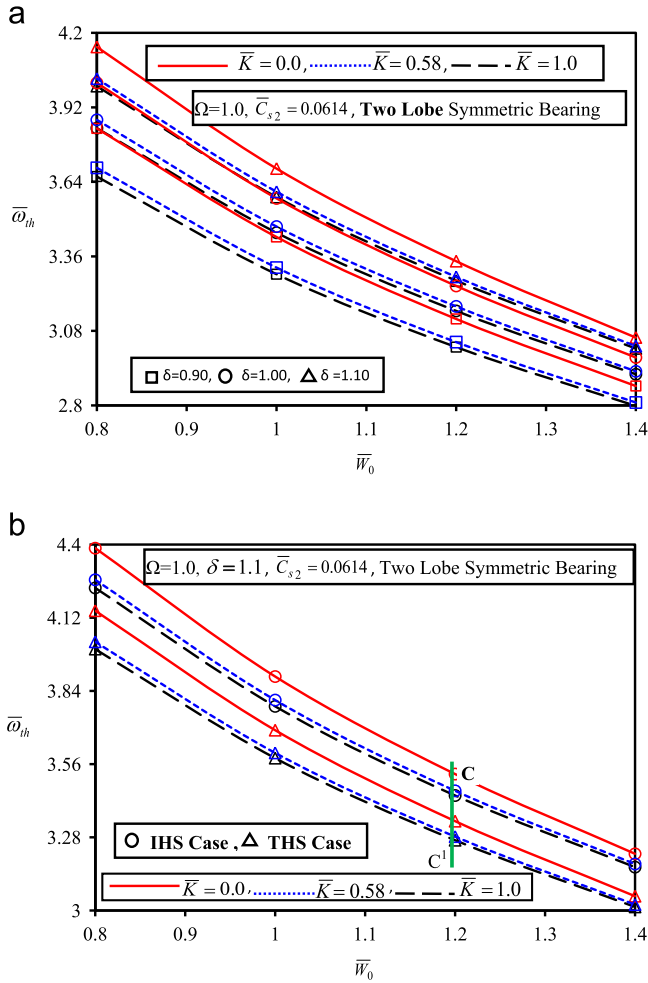


Fig. 8. (a) Variation of $\bar{\omega}_{th}$. (b) Variation of $\bar{\omega}_{th}$ for IHS and THS case.

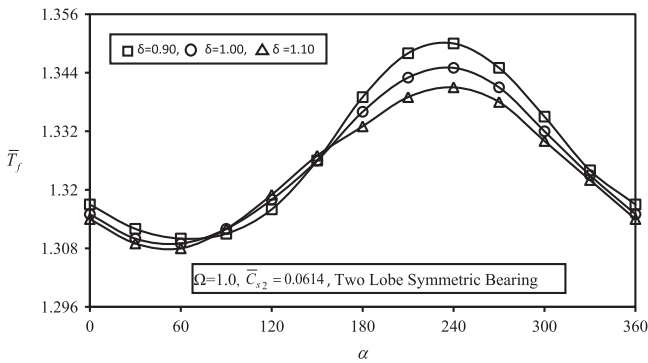


Fig. 9. Variation of fluid film temperature (\bar{T}_f).

symmetric hole entry bearing configurations. However, for a specified value of $\bar{W}_0 = 1.2$, noncircular bearing geometry $\delta > 1.0$, provides the highest value of threshold speed margin ($\bar{\omega}_{th}$).

The variation in the value of $\bar{\omega}_{th}$ for IHS (isothermal) and THS (thermal) is presented in Fig. 8(b) for 2-lobe symmetric bearing configuration. The bearing operating with cubic law lubricant at nonlinearity factor $\bar{K} = 1.0$; shows deterioration in the value of $\bar{\omega}_{th}$ and shows a maximum reduction of the order of 14.19% in THS (thermal) than that of IHS (isothermal) condition for Newtonian lubricant. This trend is anticipated in the value of $\bar{\omega}_{th}$ as it is a function of dynamic coefficients. The result of influence of nonlinearity factor $\bar{K} = 1.0$ for non-circular bearing geometry is to decrease the value of $\bar{\omega}_{th}$ by 4.69% for THS case. The value of $\bar{\omega}_{th}$ for

IHS (isothermal) condition for Newtonian lubricant $\bar{K} = 0.0$ is found to be more by 7% than THS case for the same operating condition. Further, from the results presented in Fig. 8(b), it may be revealed that a proper selection of bearing configuration and nonlinearity factor may be essential for obtaining a particular value of $\bar{\omega}_{th}$.

4.5. Variation of fluid film temperature (\bar{T}_f)

The plot of variation of fluid film temperature distribution along the circumferential axial mid plane ($\beta = 0.0$) and across the mid film for symmetric 2-lobe hole entry bearing configuration for different values of offset factor is shown in Fig. 9. It may be observed that the bearing with offset factor $\delta = 0.9$ operates at higher value of fluid film temperature than that of circular and 2-lobe bearing configuration ($\delta > 1.0$). At a given specified value of external load $\bar{W}_0 = 1.1$, an increase in the value of fluid film temperature \bar{T}_f is observed of the order of 3.4% for the bearing with offset factor $\delta < 1.0$ whereas, for $\delta > 1.0$, it has been reduced by nearly 1.2%. Further, an increase in temperature of fluid film is observed for angular location between 210° and 310° . This is due to less lubricant flow at vicinity of the applied external load at increasing values of relative eccentricity. The bearing with offset factor ($\delta > 1.0$) operates at lower value of fluid film temperature because of increased lobed radial clearance than that of circular bearing configuration.

5. Conclusion

Thermohydrostatic analysis is carried out for 2-lobe symmetric hole entry hybrid journal bearing operated with cubic law lubricant. The numerically simulated results are presented to study the influence of viscosity variation due to temperature rise, nonlinear behavior of cubic law lubricant and bearing geometry. From the results and discussion presented in this paper, the following salient conclusions are drawn:

- The influence of thermal effect on 2-lobe hole entry journal bearing operated with cubic law lubricant is to reduce the value of minimum oil film thickness vis a vis isothermal (IHS) case.
- The combined influence of thermal effect and variation of viscosity (caused due to addition of additives) is to deteriorate the values of rotordynamic coefficients and stability threshold speed margin of 2-lobe non-recessed hybrid journal bearing system.
- The loss in stability threshold speed margin due to temperature rise and viscosity variation can be compensated by selecting the proper value of offset factor ($\delta = 1.1$) and nonlinearity factor ($\bar{K} = 0.0, 0.58$).
- The noncircular journal bearing with offset factor greater than one ($\delta > 1.1$) tend to reduce the temperature of the fluid film because of increased pool of lubricant in the clearance of noncircular geometry.

References

- [1] Rowe WB, Xu SX, Chong FS, Weston W. Hybrid journal bearings with particular reference to hole-entry configuration. *Tribol Int* 1982;15(6):339–48.
- [2] Rowe WB. Advances in hydrostatic and hybrid bearing technology. *Proc Inst Mech Eng C: J Mech Eng Sci* 1989;203(4):225–42.
- [3] Nagaraju T, Sharma SC, Jain SC. Influence of surface roughness on non-Newtonian thermo hydrostatic performance of a hole-entry hybrid journal bearing. *ASME J Tribol* 2007;129(3):595–602.
- [4] Awasthi RK, Sharma Satish C, Jain SC. Performance of worn non-recessed hole-entry hybrid journal bearings. *Tribol Int* 2007;40(5):717–34.
- [5] Pinkus O. Analysis of elliptical bearing. *ASME Trans* 1956;78:965–73.

- [6] Lund JW and Thomsen KK. A calculation method and data for the dynamic coefficient of oil lubricated journal bearing. In: Proceedings of ASME design engineering conference. Chicago: ASME 100118; 1978; p. 1–28.
- [7] Li DF, Choy KC, Allaire PE. Stability and transient characteristics of four multilobe journal bearing configurations. *ASME J Lubr Technol* 1980;102:291–8.
- [8] Rahmatabadi AD, Nekoeimehr M, Rashidi R. Micropolar lubricant effects on the performance of noncircular lobed bearings. *Tribol Int* 2010;43(1–2):404–13.
- [9] Ghosh MK, Satish MR. Rotor dynamic characteristics of multi lobe hybrid bearings with short sills. Part I. *Tribol Int* 2003;36(8):625–32.
- [10] Sharma Satish C, Phalle Vikas M, Jain SC. Performance of a noncircular 2-lobe multirecess hydrostatic journal bearing with wear. *Ind Lubr Tribol* 2012;64(3):171–81.
- [11] Sinhasan R, Sah PL. Static and dynamic performance characteristics of an orifice compensated hydrostatic journal bearing with non-Newtonian lubricants. *Tribol Int* 1996;29(6):515–26.
- [12] Sharma SC, Jain SC, Sinhasan R, Sah PL. Static and dynamic performance characteristics of orifice compensated hydrostatic flexible journal bearing with non-Newtonian lubricants. *Tribol Trans* 2001;44(2):242–8.
- [13] Nagaraju T, Sharma SC, Jain SC. Performance of externally pressurized non-recessed roughened journal bearing system operating with non-Newtonian lubricant. *Tribol Trans* 2003;46(3):404–13.
- [14] Nagaraju T, Sharma SC, Jain SC. Influence of surface roughness on non-Newtonian thermo hydrostatic performance of a hole-entry hybrid journal bearing. *ASME J Tribol* 2007;129(3):595–602.
- [15] Wada Sanae, Hayashi Hirtsugu. Hydrodynamic journal bearings by pseudo-plastic lubricants, Part-I theoretical studies. *Bull JSME* 1971;14(69):268–78.
- [16] Garg HC, Kumar Vijay, Sharda HB. Performance of slot-entry hybrid journal bearings considering combined influences of thermal effects and non-Newtonian behavior of lubricant. *Tribol Int* 2010;43:1518–31.
- [17] Kushare Prashant B, Sharma Satish C. A study of two lobe non recessed worn journal bearing operating with non-Newtonian lubricant. *Proc Inst Mech Eng J: J Eng Tribol* 2013;227(12):1418–37.
- [18] Kushare Prashant B, Sharma Satish C. Nonlinear transient stability study of two lobe symmetric hole entry worn hybrid journal bearing operating with non-Newtonian lubricant. *Tribol Int* 2014;69:84–101.
- [19] Sharma Satish C, Yadav Suarabh K. Performance of hydrostatic circular thrust pad bearing operating with Rabinowitsch fluid model. *Proc Inst Mech Eng J: J Eng Tribol* 2013;227(11):1272–84.
- [20] Dowson D, Hudson J, Hunter B, March C. An experimental investigation of the thermal equilibrium of steadily loaded journal bearings. *Proc Inst Mech Eng* 1966;181(3B):70–80.
- [21] Ferron J, Frene J, Boncompain R. A study of thermohydrodynamic performance of a plain journal bearing comparison between theory and experiments. *Trans ASME J Lubr Tech* 1983;105:422–8.
- [22] Prasad Har. The effects of viscosity and clearance on the performance of hydrodynamic journal bearings. *Tribol Trans* 1988;31(2):303–9.
- [23] Khonsari MM, Jang JY, Fillon M. On the generalization of thermohydrodynamic analyses for journal bearings. *ASME J Tribol* 1996;118(3):571–9.
- [24] Sinhasan R, Chandrawat HN. Analysis of a two-axial-groove journal bearing including thermoelastohydrodynamic effects. *Tribol Int* 1989;22(5):347–53.
- [25] Banwait SS, Chandrawat HN. Study of thermal boundary conditions for a plain journal bearing. *Tribol Int* 1998;31(6):289–96.
- [26] Fillon M, Bouyer J. Thermo hydrodynamic analysis of a worn plain journal bearing. *Tribol Int* 2004;37(2):129–36.
- [27] Kumar V, Sharma SC, Jain SC. On the stability margin of hole-entry hybrid journal bearings considering viscosity-temperature variation. *Tribol Trans* 2003;46(3):421–7.
- [28] Sharma RK, Pandey RK. Effects of the temperature profile approximations across the film thickness in thermohydrodynamic analysis of lubricating films. *Ind J Tribol* 2007;2(1):27–37.
- [29] Garg HC, Kumar Vijay, Sharda HB. A comparative thermal analysis of slot-entry and hole-entry hybrid journal bearings lubricated with non-Newtonian lubricant. *ASME J Tribol* 2010;132:041701–11.
- [30] Garg HC, Kumar Vijay, Sharda HB. Performance of slot-entry hybrid journal bearings considering combined influences of thermal effects and non-Newtonian behavior of lubricant. *Tribol Int* 2010;43(8):1518–31.
- [31] Dowson D. A generalized Reynolds equation for fluid film lubrication. *Int J Mech Eng Sci* 1962;4(2):159–70.
- [32] Singh DV, Sinhasan R, Nair KP. Elastothermohydrodynamic effects in elliptical bearings. *Tribol Int* 1989;22(1):43–9.
- [33] Sharma Satish C, Kushare Prashant B. Two lobe non-recessed roughened hybrid journal bearing – a comparative study. *Tribol Int* 2015;83:51–68.
- [34] Garg HC, Kumar V. Thermohydrostatic rheological analysis of constant flow valve compensated multiple hole-entry hybrid journal bearings. *Ind Lubr Tribol* 2014;66(2):244–59.